

THE MG II CROSS-SECTION OF LUMINOUS RED GALAXIES

DAVID V. BOWEN¹ AND DORON CHELOUCHE²
(Received April 11, 2010; Accepted November 16, 2010)
Draft version June 22, 2022

ABSTRACT

We describe a search for Mg II $\lambda\lambda 2796, 2803$ absorption lines in *Sloan Digital Sky Survey* (SDSS) spectra of QSOs whose lines of sight pass within impact parameters $\rho \sim 200$ kpc of galaxies with photometric redshifts of $z = 0.46 - 0.6$ and errors $\Delta z \sim 0.05$. The galaxies selected have the same colors and luminosities as the Luminous Red Galaxy (LRG) population previously selected from the SDSS. A search for Mg II lines within a redshift interval of ± 0.1 of a galaxy's photometric redshift shows that absorption by these galaxies is rare: the covering fraction is $f(\rho) \simeq 10 - 15\%$ between $\rho = 20 - 100$ kpc, for Mg II lines with rest equivalent widths of $W_r \geq 0.6 \text{ \AA}$, falling to zero at larger ρ . There is no evidence that W_r correlates with impact parameter or galaxy luminosity. Our results are consistent with existing scenarios in which cool Mg II-absorbing clouds may be absent near LRGs because of the environment of the galaxies: if LRGs reside in high-mass groups and clusters, either their halos are too hot to retain or accrete cool gas, or the galaxies themselves — which have passively evolving old stellar populations — do not produce the rates of star formation and outflows of gas necessary to fill their halos with Mg II absorbing clouds. In the rarer cases where Mg II is detected, however, the origin of the absorption is less clear. Absorption may arise from the little cool gas able to reach into cluster halos from the intergalactic medium, or from the few star-forming and/or AGN-like LRGs that are known to exist.

Subject headings: galaxies: elliptical and lenticular, cD — galaxies: halos — galaxies: groups: general — galaxies: clusters: general — quasars: absorption lines

1. INTRODUCTION

Red galaxies contain the bulk of all the stellar mass that exists in the local Universe (Hogg et al. 2002), and thus mark the conclusion of both the dominant star formation processes, and of the assembly of galaxies. The Luminous Red Galaxies (LRGs) are a population selected by their optical colors to contain old, passively evolving stellar populations at intermediate redshift. The first two principal samples of LRGs were constructed from the *Sloan Digital Sky Survey* (SDSS; York 2000) for galaxies at redshifts $z \approx 0.2 - 0.4$ (Eisenstein et al. 2001), and from the *2dF-SDSS LRG And QSO* (2SLAQ) survey (Cannon et al. 2006) for galaxies at $z \approx 0.4 - 0.7$. Subsequently, the properties of the LRGs have been investigated by many authors: LRGs have luminosities $L > L^*$ and large stellar masses $M \gtrsim 10^{11} M_\odot$ (Banerji et al. 2010); the majority of LRGs show spectral energy distributions (SEDs) with little evidence for on-going star formation (Roseboom et al. 2006); they reside in dark matter (DM) halos with masses $M \simeq 10^{13-14} M_\odot$ (Mandelbaum et al. 2006), and in Halo Occupation Distribution (HOD) models, most LRGs are central galaxies dominating the DM halos (e.g. Zheng et al. 2009, and refs therein); they appear to be most prevalent in clusters (Ho et al. 2009). At $z \sim 0.2 - 0.8$, the evolution of the LRG luminosity function (LF) is found to be consistent with a mode in which stars form at high- z , and evolve passively thereafter with little further star formation (e.g. Wake et al. 2006; Brown et al. 2007; Cool et al. 2008; Banerji et al. 2010). It appears that these massive galaxies have already been assembled by $z \sim 1$ (Conselice et al. 2007; Ferreras et al. 2009; Banerji et al. 2010).

Given the colloquial view of LRGs as “red and dead”, they would seem an unlikely population of galaxies to harbor sig-

nificant amounts of cool gas. Nevertheless, there has recently been considerable interest in using the clustering of LRGs to infer the masses of halos in which Mg II absorption lines arise (Bouché et al. 2006; Tinker & Chen 2008; Gauthier et al. 2009; Lundgren et al. 2009, — see §4.2 for a detailed discussion of these results). The Mg II $\lambda\lambda 2796, 2803$ doublet is the first strong UV transition to be redshifted into the optical wavelength regime, at $z \gtrsim 0.2$ — a redshift low enough for galaxies responsible for the absorption to be identified. Historically, initial searches for galaxies at the same redshifts as previously identified Mg II systems were quick to confirm an association (Bergeron 1986; Yanny et al. 1987; Cristiani 1987; Bergeron & Boisse 1991; Le Brun et al. 1993). More extensive surveys suggested that all galaxies with luminosities $\sim L^*$ have absorbing cross-sections of radii $R_g \sim 60 \text{ kpc}^3$ with unity covering fraction f_c (e.g. Steidel 1993, 1995; Steidel et al. 1994). The subsequent development in numerical hydrodynamical simulations, and the refinement of semi-analytical modelling, has provided a natural explanation for multi-phase gas in galactic halos, through the inflow of baryons into regions of high density. Particularly appealing for the origin of Mg II systems are those models which describe cold flows along DM filaments, where unshocked gas at temperatures of $< 10^5 \text{ K}$ are channeled into galaxies (e.g. Kereš et al. 2009; Brooks et al. 2009; Kaufmann et al. 2009, and refs therein) at the same time that shocked gas is accreted by the halo. As Mg II absorption is thought to arise in photoionized gas with temperatures $\sim 10^4 \text{ K}$, the existence of halos with Mg II absorbing clouds is consistent with these simulations. However, one of the more important parameters governing the existence of cool gas in DM halo models is the mass of the halo. The simulations predict that in halos with masses $> 10^{13-14} M_\odot$,

¹ Princeton University Observatory, Ivy Lane, Princeton, NJ 08544.

² Department of Physics, University of Haifa, Mount Carmel, Haifa 31905, Israel.

³ Throughout this paper, we adopt $H_0 = 70 \text{ km s}^{-1} \text{ Mpc}^{-1}$, $\Omega_m = 0.3$ and $\Omega_\Lambda = 0.7$. Distances cited from published works that are originally given in units of $h^{-1} \text{ kpc}$ are converted to this cosmology.

where the LRGs reside, there should be no cool gas, whereas in lower mass halos, where the L^* galaxies mentioned above are found, there could still be enough cool gas to cause Mg II absorption along sightlines that intercept the halos (see §4.2). In these scenarios, QSO sightlines passing close to LRGs should show no Mg II absorption.

On the other hand, recent studies have focused less on the relationship of Mg II absorption and halo mass, and more on the idea that Mg II systems originate in some combination of galactic disks and starburst driven outflows. Galactic outflows offer a possible (although observationally unsubstantiated) explanation for finding cool gas clouds out to many tens of kpc from a galaxy. The fact that large-scale outflows are driven by significant star formation activity has led to more detailed investigations into the link between Mg II systems and late-type galaxies. Bouché et al. (2007), for example, showed that two-thirds of 21 sampled Mg II systems with rest equivalents widths (REWs) of $W_r > 2 \text{ \AA}$ have H α emission from galaxies with star formation rates of $1-20 M_\odot \text{ yr}^{-1}$. Zibetti et al. (2007) found excess (broad-band) emission around stacked SDSS QSO images with known Mg II systems, compared to stacked images of QSOs without absorption. The optical colors of the light suggested that the SEDs of strong Mg II absorbers are bluer than for weak ones, indicative perhaps of the domination by blue star-forming galaxies to the production of strong lines. Moreover, the large sky coverage of the SDSS, combined with the remarkable number of QSO spectra obtained, has made it possible to examine the relationship between star forming galaxies and Mg II systems, without regard to the identification of any galaxy close to the line of sight. Emission lines have been detected in QSO spectra at the same redshifts as absorption line systems, either in stacks of spectra (Wild et al. 2007; Ménard et al. 2010) or in rarer cases, individual QSO spectra (Noterdaeme et al. 2010; Borthakur et al. 2010).

Whether these results indicate that absorption arises in large-scale gaseous outflows, rather than simply from galactic disks that host star forming regions, is less clear. The idea that galactic disks are responsible for Mg II lines has long been appealing (Wagoner 1967; Bowen et al. 1995; Charlton & Churchill 1996; Steidel et al. 2002), and modeling Mg II absorbing gas as a combination of disk and outflow features, naturally explains the range of galaxy luminosities and star formation rates observed (Chelouche & Bowen 2010). The detection of low ionization optical absorption lines in outflows from nearby starburst galaxies, using the light from the galaxy itself to probe the gas (Martin 1999; Schwartz & Martin 2004; Martin 2005; Rupke & Veilleux 2005) adds support for the model, and indeed, Mg II absorption is seen from outflows of high- z galaxies (Tremonti et al. 2007; Weiner et al. 2009). Detailed investigations of starburst galaxies certainly suggest that these types of galaxies produce multi-phase outflows (Strickland et al. 2004b,a) that would show absorption lines from many different ionization states if penetrated by a QSO sightline. It remains to be seen though how ubiquitous these outflows are at higher redshift around the majority of late-type galaxies, whether QSOs lines of sight, probing in a direction transverse to galaxy sightlines, would see similar absorption signatures as those recorded towards the centers of galaxies, or, indeed, whether outflowing gas capable of producing the types of absorption seen can escape out to many tens of kpc from galaxies.

The redshifts at which Mg II becomes detectable in SDSS

spectra [and where the SDSS sensitivity allows for detection of weaker lines in higher signal-to-noise (S/N) data] is in the range $z \simeq 0.36-0.43$ (3800–4000 Å). An interest in the association between Mg II systems and LRGs arises from the fact that at these redshifts and beyond, the LRGs are, pragmatically, the only galaxies detectable in SDSS images with reliable photometric redshifts (hereafter “photo- z s”). The availability of good quality photo- z s can be used to cull a large number of faint, intermediate- z galaxies without having to first measure their redshifts through expensive, time-consuming spectroscopic surveys. If the galaxies are observed as part of a survey — such as SDSS — which also records the spectra of a similarly large number of QSOs, then the opportunity to study the absorbing properties of the galaxy ensemble is obvious. The fact that, in this particular case, such a set of galaxies happens to be LRGs, means we can explore Mg II absorbing gas in the halos of a restricted, specific, and rare type of galaxy and their environment. The theoretical considerations discussed above suggest we should find no absorption, but this paper seeks to test that prediction.

Most surveys designed to find galaxies responsible for absorption systems have been based on targeting Mg II systems known *ab initio*. While this approach yields information on the origin of the absorption, it does not necessarily define the absorbing properties of galaxies. Prior to the launch of the *Hubble Space Telescope* (HST), efforts to study the gas in disks and halos of galaxies focussed on pairing very low-redshift galaxies with QSO sightlines and searching for absorption lines (Ca II $\lambda\lambda 3933, 3968$, Na I $\lambda\lambda 5889, 58955$, etc.) that could be observed from the ground (e.g. Boksenberg & Sargent 1978; Boksenberg et al. 1980; Blades et al. 1981; Bergeron et al. 1987; Womble et al. 1990; Bowen et al. 1991). With HST, it became possible to search for the more sensitive and abundant UV lines from nearby galaxies instead. That work showed that at $z \sim 0$, there is little evidence for Mg II absorbing clouds around galaxies beyond ~ 50 kpc (Bowen et al. 1995), and when detected, the absorption originates in galactic disks (Bahcall et al. 1992; Bowen et al. 1995, 1996) or in tidal debris between the identified galaxy and an often fainter companion (Bowen et al. 1994, 1995) — even when the targeted galaxy is a known starburst (Norman et al. 1996).

Unfortunately, studies of galaxies in the local Universe are hampered by the necessity of having to use QSOs with the brightest UV continua, in order to obtain sufficient signal-to-noise with the available HST spectrographs. To avoid this limitation, and to make use of the huge number of QSO sightlines observed spectroscopically with SDSS, more aggressive attempts have been made recently [following a much earlier study by Bechtold & Ellingson (1992)] to identify galaxies at higher redshifts and to again search for Mg II lines shifted into the optical, without any prior information on the absorption lines in the background QSO spectra. The absorbing cross-section of a galaxy, R_g , and the covering fraction of the gas f_c , are obviously inter-related; if f_c declines with radius (i.e. if there is no sharp boundary to R_g), then R_g can be set arbitrarily for a given f_c , and vice versa. Similarly, both R_g and f_c can, in principle, depend on the equivalent widths of the lines. In a study using early results from SDSS, Tripp & Bowen (2005) found galaxies at $z \sim 0.3-0.6$ with f_c only $\simeq 50\%$ for $R_g \sim 50$ kpc, for sensitivities of $W_r \gtrsim 0.1 \text{ \AA}$. Similarly, for $W_r \geq 0.3 \text{ \AA}$, Barton & Cooke (2009) found $f_c \simeq 0.25-0.4$ for $R_g \simeq 110$ kpc, or $f_c \sim 0.25$ for smaller radii of $R_g \sim 50$ kpc, for galaxies at $z \simeq 0.1$. Conversely, however,

Chen et al. (2010) [see also Chen & Tinker (2008)] measured much higher covering fractions and larger cross-sections for galaxies at $z \simeq 0.2$: $R_g \simeq 110$ kpc and $f_c \simeq [0.7, 0.8]$ for $W_r \geq [0.3, 0.1] \text{ \AA}$. These radii are obviously considerably larger than the cross-sections measured for galaxies at $z \sim 0$.

One caveat to this work is that at higher redshifts, identifying the processes responsible for absorption systems is much harder. At these redshifts, galaxy features are hard to discern even in high resolution HST images, low surface brightness features are difficult to detect, multi-wavelength observations (e.g. 21 cm interferometry observations, which are important for mapping high H I column densities around galaxies) are often not possible, and the light of a background QSO masks any faint emission directly along a sightline. (Indeed, these difficulties also hamper the study described in this paper, as we discuss in §4.1.) Hence, even with more comprehensive surveys of absorbing galaxies at $z \gtrsim 0.1$, it remains difficult to know whether Mg II absorption marks gas inflowing from filaments, outflows from star-formation activity, the extension of galactic disks, the tidal debris between multiple galaxies, or some combination of all these mechanisms. Hence our current ambitions are to pre-select galaxies with defined characteristics, whose properties have been determined from understood processes, and use such calibrations to interpret the origin of the observed absorption systems.

In this paper, we study the absorbing properties of LRG galaxies — again, selected without any prior bias towards knowing whether or not Mg II exists at the redshifts of the galaxies. Our initial approach was to simply define a sample of SDSS galaxies close to QSO sightlines that had photometric redshifts with very small errors, and to search for Mg II absorption in the SDSS spectra of the background QSOs. As described below, we began such a program without regard to the type of galaxies selected. We found, however, that the selection of LRG galaxies in the SDSS arises naturally from demanding that the photo- z errors of galaxies be small. We note here that, concurrent with our investigations, Gauthier et al. (2010) have also examined the absorbing properties of a set of galaxies (with photo- z s) selected *a priori* to be LRGs. Their results, obtained independently of ours, obviously offers an important comparison with our study, and we discuss their results in §3 and §4.

The outline of this paper is as follows: in §2.1 we define how we selected the galaxies to study, and describe the search for Mg II at their redshifts in §2.2. In §2.3 we describe the properties of the galaxies, and demonstrates why the majority of them are LRGs. We discuss the results of the study in §3, and their implications in §4.

2. SAMPLE SELECTION

2.1. Selection of galaxies with photometric redshifts

We began an investigation of galaxies close to SDSS QSOs with no regard to the properties of the galaxies themselves. That is, there was no initial aim of selecting only LRG galaxies in our study. We aimed to utilize both the photometric redshift information that was available for SDSS galaxies, and existing high quality spectra of SDSS QSOs. Only after forming a suitable sample of QSO-galaxy pairs did it become clear that the galaxies were LRGs. We discuss the properties of the galaxies in our sample more fully in §2.3. In this section, we describe the criteria that were actually used to select galaxies close to QSOs.

We first compiled a list from DR6 of QSOs observed spec-

troscopically by SDSS, and which had galaxies within 30 arcsec of the QSO sightline⁴ that also had cataloged photometric redshifts. We imposed a basic cutoff for the photo- z of a galaxy to be $z_{CC2} > 0.4$ (see below for a definition of this quantity), $z_{CC2} < z_{QSO}$, and a galaxy morphology (“type” = 3). The minimum photo- z of $z_{CC2} = 0.4$ was imposed since Mg II was not expected to be readily detectable below $\simeq 3900 \text{ \AA}$ in SDSS spectra (see below). This basic selection yielded a sample of $\sim 80,000$ pairs.

The most important criterion in selecting a suitable subset of galaxies for which we would search for Mg II absorption, was that the photo- z should be reliable — that is, the photo- z error should be small. The SDSS database contains two measures of a galaxy’s photo- z estimated from the work of Oyaizu et al. (2008), tagged in the SDSS database as “D1” and “CC2” (which we refer to as z_{D1} and z_{CC2}) both neural network based estimators. z_{D1} uses galaxy magnitudes in the photo- z fit, while z_{CC2} uses only galaxy colors. Each of these photo- z estimates have errors associated with them (based on an empirical “Nearest Neighbor Error” method), although there are two measurements of the error in each case, because the distribution of errors $\Delta z = |z_{\text{phot}} - z_{\text{spec}}|$ — the difference between the photo- z and the real redshift of a galaxy in a training set of galaxies — are non-Gaussian. There are two estimates in the error of the photo- z s: one error is given by σ_{68} , which contains 68% of the values of Δz in the training sample; the other, which we call σ_{rms} (simply “ σ ” in Oyaizu et al.), is the rms scatter (again, see Oyaizu et al. for more details).

The accuracies of CC2 and D1 decline quickly for r -band galaxy magnitudes fainter than $r = 20.0$. The majority of galaxies found close to QSOs in our initial search for QSO-galaxy pairs had $r > 20.0$, and excluding these would result in a sample too small to be of interest. Based purely on galaxy magnitude, the errors in z_{D1} and z_{CC2} rise sharply from 0.05 to 0.09 between $20.0 < r < 21.0$ (see Fig. 5 of Oyaizu et al.). Fortunately, for the galaxy redshifts we are interested in — at $z > 0.4$ — photo- z s are defined to a high accuracy as the 4000 \AA break in the galaxy spectra passes through the r -band. Figure 6 of Oyaizu et al. shows that between $z = 0.4 - 0.6$, σ_{68} for z_{CC2} ranges from $\simeq 0.04 - 0.09$, and is smaller than σ_{rms} by $\Delta z \approx 0.02$. In this paper, we adopt σ_{68} as the error we use, and denote this simply as $\sigma(z)$.

We interpret these results to mean that, for 68% of selected QSO-galaxy pairs, the true redshift of the galaxy lies between $z_{\text{phot}} - \sigma(z)$ and $z_{\text{phot}} + \sigma(z)$. From our original collation of galaxy pairs, we therefore selected only galaxies with $\sigma(z) \leq 0.05$. We took the maximum photo- z to be 0.6, while the minimum photo- z was not determined by the photometric properties of the galaxies themselves, but by the minimum wavelength that Mg II could be detected in SDSS spectra. We took this minimum to be 3800 \AA , plus a redshift path which allowed a search for Mg II within $2\sigma(z)$ (see below). The resulting minimum redshift was 0.46. Given this redshift range, and the 30 arcsec limit for finding galaxies, the maximum impact parameters studied are between 175 and 201 kpc.

To further reduce including galaxies with spurious photo- z s, we also demanded that $|z_{CC2} - z_{D1}| < \sigma(z)$, i.e. that the photo- z s estimated from the two different methods agreed to within 1σ of each other. Additional constraints included: $z_{QSO} - z_{CC2} > 0.3$, to avoid Mg II associated with the QSO itself; and $z_{QSO} <$

⁴ i.e. objects which are identified as “neighbors” to QSOs in the specObj view of the SDSS database

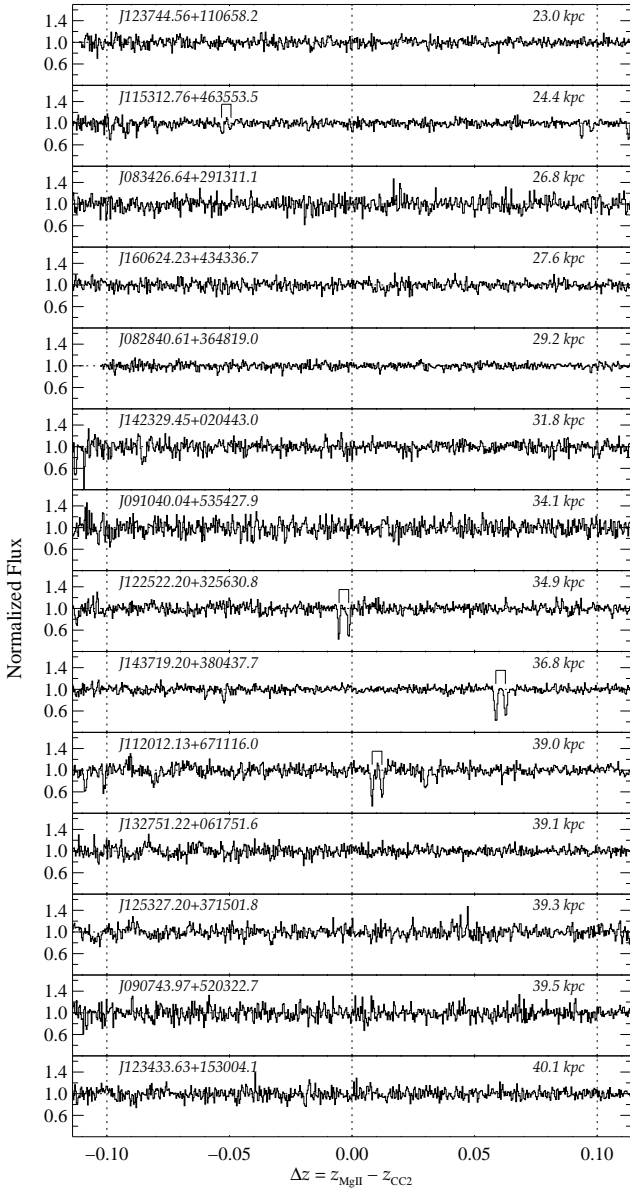


Figure 1. Representative normalized spectra of QSOs in our sample with sensitivities $2\sigma(W) < 0.4 \text{ \AA}$. Spectra are selected for QSOs that have the 14 closest galaxies, with the impact parameter ρ printed at the top right of each panel. The x-axis shows the wavelength reduced to a redshift range for Mg II $\lambda 2796$, and normalized to z_{CC2} . The QSO designation is given at the top left of each panel. Mg II, when detected, is marked with two vertical bars. The dotted lines at $\Delta z = \pm 0.1$ represent the range over which Mg II was searched for.

2.1, to exclude high- z Ly α -forest lines in the SDSS spectra. In a few cases, more than one galaxy satisfying all these criteria was found in a single QSO field; these galaxies were flagged and are discussed later.

Further culling of the original sample was made based on the spectroscopic properties of the background QSOs. These are discussed in the next section.

2.2. The search for Mg II absorption from foreground galaxies

For the QSO-galaxy sample described above, formed from criteria applied to galaxies, we next considered a set of criteria

based on the suitability of the QSO spectra. We first rejected all QSOs with signal-to-noise (S/N) ratios in the continuum of less than 6.0 per pixel at z_{CC2} , based on the error arrays generated from the pipeline extraction of the one-dimensional SDSS spectra. At $z \simeq 0.5$, this S/N corresponds to a 3σ rest-frame equivalent width (REW) limit of $W_r \approx 0.7 \text{ \AA}$ (when calculated using the method described below). We rejected spectra with extraction defects, Broad Absorption Line complexes, complicated continua, or those contaminated by complex and numerous higher- z systems. In some cases, we rejected spectra where Mg II was expected to fall close to a particularly sharp QSO emission line, since defining the continuum at the peak of these emission lines can be difficult (particularly in cases where associated absorption lines are seen superimposed on the emission line).

For the accepted spectra, we normalized the QSO continua by defining a least-squares fit of Legendre polynomials to the continuum flux (Sembach & Savage 1992). For each spectrum, we then calculated an array of observed $2\sigma(W_i)$ equivalent widths (EWs), where, at each pixel i , $\sigma^2(W_i) = \sum_i^n (\sigma_i \delta\lambda)^2$, and $\delta\lambda$ is the wavelength dispersion in \AA pixel^{-1} . Error arrays from the SDSS pipeline again provided values of σ_i , and we took n to be a value twice the resolution expected for SDSS spectra⁵, or five pixels.

In each normalized QSO spectrum, we searched for Mg II absorption within a window of $\pm 2\sigma(z)$ of z_{CC2} , i.e. $\Delta z = \pm 0.1$. Using a value of $\pm 2\sigma(z)$ corresponds conveniently to assuming that $\approx 95\%$ of the LRG photo- z s will be correct; if we had chosen to use σ_{rms} instead of σ_{68} , we would have to have increased the path length by $\delta z \approx \pm 0.04$ to include $\pm 2\sigma_{\text{rms}}$. Reviewing the SDSS QSO spectra used in our survey indicates that one more Mg II system would have been detected if we had adopted this estimate of the photometric redshift errors. As we shall see below, this would have made little difference to the final results.

Detection of Mg II required that both members of the doublet be found with EWs $> 2\sigma(W_i)$, although only the Mg II $\lambda 2796$ line had to lie in the $\pm 2\sigma(z)$ window. When detected, we fitted Gaussian profiles to the lines and calculated a final redshift for the absorption system by averaging the redshifts measured for each line of the doublet. Line equivalent widths were measured in the standard way, $W = \sum_i^n (1 - F_i) \delta\lambda$, where F_i is the normalized flux at the i 'th pixel, and the sum is calculated over n pixels. As noted above, for unresolved lines, $n = 5$. However, many strong Mg II lines found in SDSS spectra have widths that are larger than this; in order not to underestimate W therefore, for lines detected with EWs $> 6\sigma(W_i)$ (i.e. lines defined with high S/N), we increased n to cover a width of $\pm 3\sigma_{\text{gauss}}$, where σ_{gauss} was the width of the Gaussian profile fitted to a line.

Were the redshift of a galaxy to be measured spectroscopically, the 2σ EW limit for Mg II if a doublet was *not* detected would be given by the value of $2\sigma(W_i)$ at the appropriate wavelength. In order to define an equivalent width limit over a wavelength range corresponding to $\pm 2\sigma(z)$, however, we need to be sensitive to lines with EWs greater than some EW limit over the entire range of $\pm 2\sigma(z)$. We therefore define the 2σ REW limit, W_{lim} , to be the maximum value of $2\sigma(W_i)$ in the EW array between $\pm 2\sigma(z)$, after each point in the EW array is corrected to be in the rest frame of $z_i = \lambda_i/\lambda_0 - 1$ (where

⁵ At the wavelengths where Mg II is expected the resolution of the SDSS spectra is $\simeq 2.2 \text{ \AA}$ at 4500 \AA , FWHM, or $\sim 150 \text{ km s}^{-1}$.

λ_0 is the wavelength of the Mg II $\lambda 2796$ line). For SDSS spectra, $\sigma(W_i)$ is relatively flat as a function of wavelength over the redshift range considered here, so is close to the value that would be calculated at exactly z_{CC2} .

Examples of the spectra used in our survey are shown in Figure 1. For this figure, the QSOs chosen are sorted by QSO-galaxy impact parameter, and we have only selected spectra with sensitivities of $W_{\text{lim}} \leq 0.4 \text{ \AA}$, simply to highlight better quality data. Figure 2 shows color representations of the fields around these QSOs. Each image is a cutout extracted from the SDSS database, and so is a g -, r -, and i -band composite of the original imaging data (Lupton et al. 2004). Full details on all the pairs selected are given in Table 1; the table includes details of the QSOs and galaxies in the sample, as well as the results from the search for Mg II absorption: values of REWs when Mg II was detected, or limits when the lines were not detected, are listed therein.

2.3. Galaxy Properties

In Figure 3 we plot the $g-r$ and $r-i$ colors of the galaxies in our sample. Even though the colors of galaxies were not used in their selection, their distribution in the color diagram is confined to a narrow region with $1.5 \leq g-r \leq 2.0$ and $0.7 \leq r-i \leq 1.2$. These colors are similar to those used by Eisenstein et al. (2001) and Cannon et al. (2006) to define LRGs at the same redshifts as the galaxies in our sample. The reason these authors applied such color cuts initially, and the reason for expecting their surveys to focus on $z \sim 0.2-0.5$ early type galaxies, was because the SEDs of such galaxies are predicted to fall above specific color cuts. So, for example, Figure 3 shows the cuts, designated d_{\perp} and c_{\parallel} , used by Cannon et al. to define spectroscopic targets in the 2SLAQ sample. They defined d_{\perp} to select early type galaxies at increasingly higher redshifts, and c_{\parallel} to eliminate late-type galaxies altogether. In the figure, we have drawn a line for $d_{\perp} = 0.55$, which defined ‘‘sample 3’’ of the galaxies studied by Cannon et al., and which contained the bulk of their LRG sample. Most of the galaxies we selected lie in the same color region as their LRGs.

The way in which the SEDs of early-type galaxies produce different broad-band colors as a function of redshift is well understood. A change in the $g-r$ color to a constant value at $g-r \simeq 1.7$ measures the transition of the 4000 \AA break in a galaxy’s SED as it moves from the g -band to the r -band at $z \sim 0.4$; $g-r$ begins to increase again at $z = 0.7$ as the 4000 \AA break moves into the i -band. To demonstrate this effect, we have used the LRG SED provided by Blanton & Roweis (2007) to show how the colors change with z when convolved with SDSS filters. These are shown as red circles in Figure 3, where a circle is plotted every $\delta z = 0.02$ up to $z = 0.6$. We have also plotted the expected colors of a late-type Sbc and Scd galaxy using the SEDs of Coleman et al. (1980), as green and orange circles, respectively.

Figure 3 shows that the colors of the galaxies in our sample are largely consistent with early-type LRG colors, and not with late-type galaxies. More sophisticated modeling shows that theoretical SEDs can also reproduce these colors, assuming stars formed in a single burst 11 Gyr ($z \sim 2.5$) ago and with a star formation time scale of 1–3 Gyr (Banerji et al. 2010, and refs. therein).

Hence the majority of the galaxies in our sample are early-type LRG galaxies. The reason for principally selecting LRGs is almost certainly because these types of galaxies, with a well defined 4000 \AA break, provide the most accurate photo- z -es-



Figure 2. Representations of some of the SDSS QSO-galaxy pairs used in this survey. The fields shown include those with QSO spectra plotted in Figure 1; they thus represent the pairs with the smallest impact parameters, and with $W_{\text{lim}} \leq 0.4 \text{ \AA}$ for the QSO spectra. Each image is 60 arcsec on a side, with NE to the top-left. Although not labeled, the impact parameters between QSO sightlines and galaxies are between 20.0 (top left corner image) and 40.0 kpc (bottom right corner image). Full details can be found in Table 1. The QSO designation is printed at the top of each image, and its position is indicated by cross-hairs. Cross-hairs in red represent QSOs that show Mg II near the photo- z of the galaxy, while white cross-hairs indicate that no absorption was detected. Galaxies are identified by arrows, and always lie at the center of the field.

timates. Since we selected galaxies based on small values of $\sigma(z)$, we therefore predominantly picked galaxies with the strongest Balmer breaks.

We can compare the luminosities of the galaxies in the sample with those of the LRG population. By adopting the same LRG SEDs discussed above, we can derive suitable K -corrections to apply to our galaxies and thereby estimate accurate absolute magnitudes M . These corrections are necessary, since the values needed to correct, for example, M_r derived from r -band observations, and the true rest-frame M_r is $K_r \sim 0.9-1.4$ for $z = 0.46-0.6$. The luminosity function (LF) for LRGs at intermediate redshift has been derived by Wake et al. (2006), and is reproduced in Figure 4. The blue points

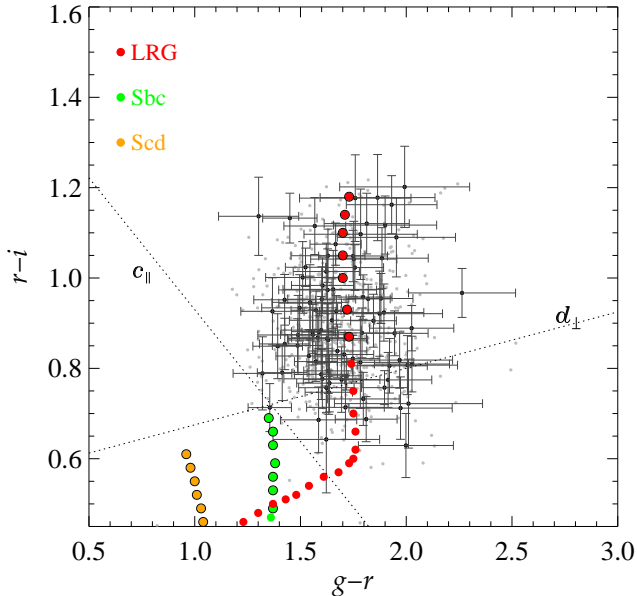


Figure 3. Plot of broad-band colors for galaxies in our selected sample of QSO-galaxy pairs. Black circles represent galaxies for which Mg II was detected within $\delta z \pm 0.1$ of the photo- z of the galaxy, z_{CC2} ; gray circles represent non-detections of Mg II. To avoid confusion, errors in the colors are shown only for Mg II detections, and not for Mg II non-detections. Also shown are theoretical colors for a Luminous Red Galaxy (LRG, in red), an Sbc (green) galaxy, and an Scd (orange) galaxy, calculated over redshift intervals of 0.02. The last points plotted are for $z = 0.6$, and for emphasis, the redshifts corresponding to the criterion used to select galaxies, $z_{CC2} = 0.46 - 0.6$, also have black outlines around the circles. The color cuts used by Cannon et al. (2006) are shown as dotted lines, and are $c_{\parallel} = 0.7(g-r) + 1.2(r-i - 0.18) \geq 1.6$, and $d_{\perp} = (r-i) - (g-r)/8.0 > 0.55$ (see text).

represent the volume density of LRGs at $0.5 < z < 0.6$ taken from the 2SLAQ, corrected for passive evolution as well as including K -corrections. In this case, the corrections to the absolute magnitudes $M_{0.2r}$ are made to measure the luminosity at $z = 0.2$. Making the same correction, but not including an evolutionary correction (which is much smaller than K_r), we measure the distribution of $M_{0.2r}$ for the galaxies in our sample and plot them as a histogram in Figure 4. The actual normalization of the histogram is not relevant here: the figure simply demonstrates that the galaxies have largely the same distribution of luminosities as the LRG population.

For the final sample of galaxies, we searched for existing (DR7) SDSS spectra of the galaxies, in order to confirm both their photometric redshifts and the shape of their SEDs. Only two spectra were available, for two galaxies at distances of more than 144 kpc from their background QSO sightlines, neither of which were associated with any Mg II absorption lines. The S/N of both spectra were very poor, and insufficient to provide accurate redshifts. Given the limit of the SDSS MAIN galaxy sample, $r = 17.8$, and the extended LRG sample, $r = 19.2$ (Eisenstein et al. 2001), we would expect very few of our galaxies to have been observed spectroscopically: our sample consists of only [0,0.3]% of galaxies brighter than $r = [17.8, 19.2]$.

3. RESULTS

Having applied all the selection criteria discussed in §2.1, the final sample consisted of 593 QSO-galaxy pairs. There are 26 galaxies that have another galaxy with a photo- z lying closer to the QSO sightline, or, 23 galaxies that have another

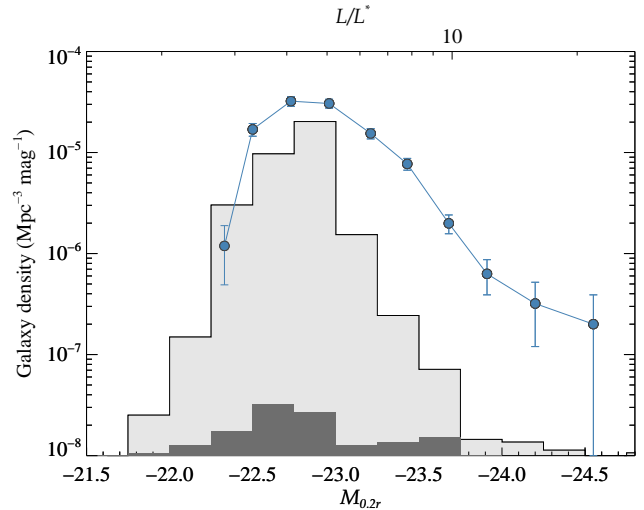


Figure 4. Plot of the r -band luminosity function of LRGs normalized to $z = 0.2$ taken from Wake et al. (2006) (blue line). In order to compare the absolute magnitudes of the galaxies in our QSO-galaxy pairs sample, we overplot a histogram (light gray) line for all the galaxies selected. The normalization of the histogram is arbitrary, but shows that the galaxies in our sample have similar luminosities to the LRG samples. The distribution of absolute magnitudes of galaxies which show Mg II absorption are plotted in dark gray. The top x-axis shows the ratio of L/L^* assuming $M_*^* + 5 \log h = -20.4$ (Blanton et al. 2003) and no evolution in the LRG LF between $z = 0.1 - 0.2$.

galaxy with a photo- z lying closer to the QSO sightline and for which the background QSO spectrum has $W_{\text{lim}} < 0.6 \text{ \AA}$. For the remainder of this section, we exclude galaxies further away than another closer identified galaxy (with a photo- z), but we reconsider if their exclusion is warranted in §4.1. Of the 567 remaining galaxies, [175,42] have impact parameters of $\rho \leq [100,50]$ kpc. At these separations, we found Mg II absorption within $\Delta z = \pm 0.1$ of the galaxies' z_{CC2} in [41,9] cases. Representative spectra have already been shown in Figure 1. Of the 89 detections of Mg II absorption (at all radii), 11 spectra showed 2 or 3 Mg II systems within the search window. This number is too small to infer anything about the clustering of Mg II systems in this sample, and more comprehensive discussions on the cross-correlation between Mg II systems and LRGs have been given by Bouché et al. (2006) and Tinker & Chen (2008). In this paper, we select the system with the redshift closest to the photo- z of the LRG as the one “associated” with the galaxy or its environment.

The REWs, W_r , for detected Mg II $\lambda 2796$ lines, or 2σ REW limits W_{lim} when no lines were detected, are plotted against galaxy impact parameter ρ in Figure 5. For each ρ , there is an uncertainty $\sigma(\rho)$ caused by not exactly knowing the redshift of the galaxy. This error is small though, since $|\sigma(\rho)| = 2\rho\sigma(z)/(1+z)^2$, which is only 7% of ρ for $\sigma(z) = 0.05$ at $z = 0.5$. These errors are omitted in Figure 5. The figure shows that the equivalent width limit of the survey is $\lesssim 0.7 \text{ \AA}$, as expected from selecting QSO spectra with a minimum S/N ratio. That is, we were able to always detect any Mg II lines with $W_r > 0.7 \text{ \AA}$. In many cases of course, the spectra were sensitive to detect lines much weaker than this, down to $W_r \gtrsim 0.2 \text{ \AA}$. Also as expected, galaxy impact parameters extended out to ≈ 200 kpc, the limit imposed by selecting galaxies within 30 arcsec of a QSO sightline. Mg II lines are detected up to REWs of $W_r \approx 2 \text{ \AA}$, but there is no correlation

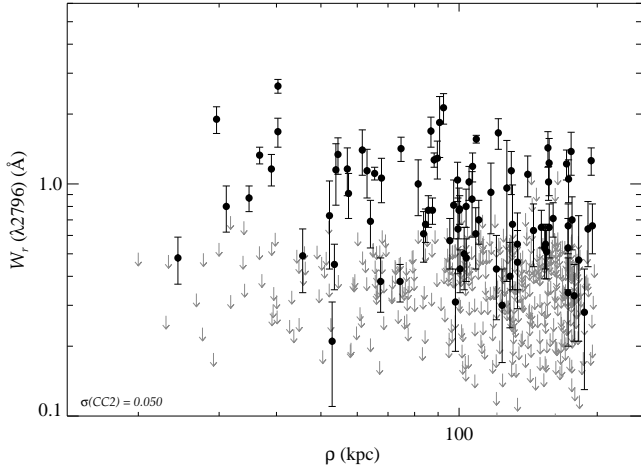


Figure 5. Mg II $\lambda 2796$ Rest equivalent width W_r , or 2σ limits, plotted against QSO-galaxy impact parameter ρ .

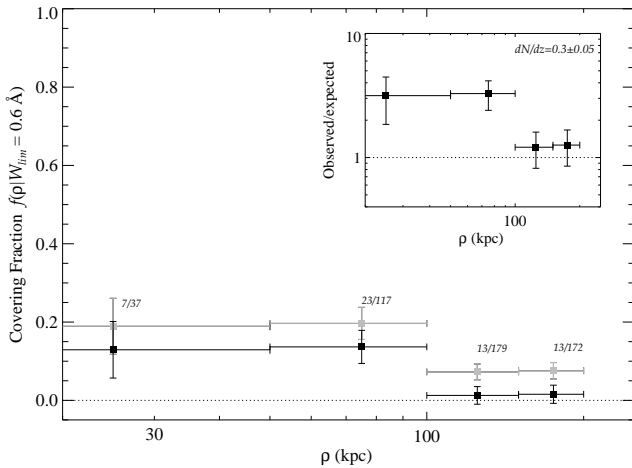


Figure 6. Plot of the covering fraction $f(\rho)$ for galaxies in the sample, plotted against QSO-galaxy impact parameter ρ . The gray squares represent $f(\rho)$ without any corrections for the chance detection of an Mg II system along a sightline; the fraction of detections to total number of pairs in each bin [which defines $f(\rho)$] is written next to each point. The black squares represent $f(\rho)$ after subtracting the predicted number of chance detections, assuming $dN/dz = 0.3$ at $z \simeq 0.5$. Horizontal error bars show the adopted bin sizes. If some of the absorption detected does not actually arise from the probed LRGs, but, e.g., from companion galaxies, then the points drawn here (and in Fig. 7) represent only upper limits to $f(\rho)$ for LRGs (see §4.1). *Inset:* The ratio of the observed number of Mg II systems to the expected number, again assuming $dN/dz = 0.3$.

of W_r with ρ . In particular, there are many sightlines that show *no* Mg II to REW limits of 0.2–0.7 Å. Figure 3 demonstrates that Mg II detections are not a function of galaxy color, since detections are found for all values of $g-r$ and $r-i$ colors in the sample.

The covering fraction of galaxies, $f(\rho)$, is defined simply as the number of galaxies with detected Mg II at some impact parameter, compared to the total number of galaxies. To calculate $f(\rho)$, it is necessary to use an equivalent width limited sample of sightlines. To that end, we selected only sightlines with S/N ratios high enough to reach REW limits ≤ 0.6 Å,

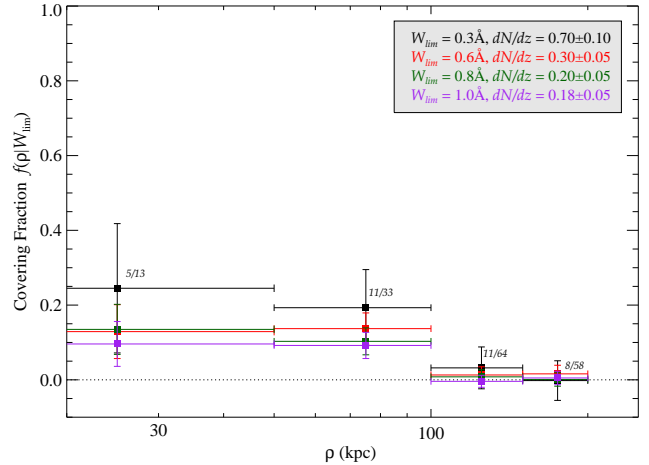


Figure 7. Plot of the covering fraction $f(\rho)$ for different values of W_{lim} , after correcting for the predicted number of Mg II absorbers along the QSO sightlines. For the $W_{\text{lim}} = 0.3$ Å sample alone (shown with black points), the ratio of the number of detections to the total number of sightlines selected, is indicated as a fraction next to each point. The legend in the top right corner matches the color of the points to the W_{lim} adopted in calculating $f(\rho)$, and shows the values of dN/dz used to correct the observed fraction of detections to non-detections.

irrespective of whether Mg II was detected or not. This meant that the selected spectra could detect lines as strong as, or stronger than, 0.6 Å. Since the highest S/N spectra in such a sample could also detect lines weaker than 0.6 Å, we only counted a detection if it too had a REW ≥ 0.6 Å. Hence the covering fractions include sightlines where we *could* have detected lines with REW ≥ 0.6 Å, and where $W_r \geq 0.6$ Å when a line was detected. The results are shown in Figure 6, where values for $f(\rho)$ are plotted as gray squares. Error bars are taken to be simply Poissonian errors on the number of detections. The covering fraction is consistently low, starting at 0.2 between $\rho = 24-50$ kpc, and declining to 0.1 between $\rho = 150-200$ kpc.

Although we detect Mg II within $\pm 2\sigma(z)$ of z_{CC2} towards some galaxies, in order to properly measure $f(\rho)$, we must also consider how many of the Mg II detections arise simply from chance. The number of Mg II absorbers per unit redshift, dN/dz , is given by Nestor et al. (2005), and at $z = 0.5$ is $\simeq 0.3$ for $W_r > 0.6$ Å. From their work, we estimate an error in $dN/dz \simeq 0.05$, and include this in computing the error bars in Figure 6. Over a given redshift interval, we can therefore calculate the number of Mg II absorbers expected to arise by chance and subtract these from the number of detections. The resulting values are shown as black squares in Figure 6. The ratio of the observed number of systems to the expected number is also shown inset to Figure 6. The figure shows that $f(\rho)$ is small but non-zero at $\rho < 100$ kpc, but that beyond this, $f(\rho)$ is consistent with zero. This implies that any detection of Mg II beyond $\rho > 100$ kpc is probably just from chance, and that the galaxies selected in this sample have no associated Mg II absorption beyond 100 kpc.

We initially selected an REW limit of 0.6 Å for two reasons: first, because it lies close to the median of the REW distribution in our sample, and would therefore allow us to include a significant number of spectra; and second, because a value of dN/dz for that limit was available in the literature. In their search for Mg II from a sample of galaxies de-

finned to be LRGs, Gauthier et al. (2010) calculated a covering fraction for lines with a REW of 0.5 \AA , a value similar to ours. They found $f(\rho) \sim 20\text{--}40\%$ for $\rho \lesssim 100 \text{ kpc}$, and a largely constant (with some deviations) $f(\rho)$ of $\sim 20\%$ between $\rho \simeq 100\text{--}400 \text{ kpc}$. This result is clearly different from our measurement of a sharp decline of $f(\rho)$ to approximately zero beyond 100 kpc .

Gauthier et al. (2010) also calculated $f(\rho)$ for much stronger lines, those with REW limits $> 1.0 \text{ \AA}$, and found a factor of ≈ 2 smaller $f(\rho)$ than for their analysis using REWs limits of 0.5 \AA . We can see whether any differences in $f(\rho)$ exist for different REW limits in our sample. Since we are primarily interested in $f(\rho)$ after correcting for Mg II lines that might arise by chance in our Δz window, we need to know dN/dz at these REW limits. For W_{lim} greater than 0.6 \AA , we can use values of dN/dz computed by Nestor et al. (2005) and Lundgren et al. (2009) of $dN/dz = 0.2$ and 0.18 for $W_{\text{lim}} = 0.8$ and 1.0 \AA , respectively. Again, $f(\rho)$ depends weakly, but non-negligibly, on the error in dN/dz , so we have estimated an uncertainty of ≈ 0.05 in dN/dz . The results are shown in Figure 7. For $W_{\text{lim}} = 0.6\text{--}1.0 \text{ \AA}$, $f(\rho)$ is largely the same, reaching between $10\text{--}15\%$ for $\rho < 100 \text{ kpc}$, then falling sharply at larger ρ .

We can also estimate $f(\rho)$ for $W_{\text{lim}} < 0.6 \text{ \AA}$. Nestor et al. measure $dN/dz \simeq 0.7$ for $W_{\text{lim}} = 0.3 \text{ \AA}$, although the error on this value appears to be larger than for the other values of dN/dz — we estimate an error of ≈ 0.1 . Figure 7 shows that at this REW limit, $f(\rho)$ may be perhaps as much as a factor of two larger at $\rho < 100 \text{ kpc}$, although it too falls to zero quickly at $\rho > 100 \text{ kpc}$. Unfortunately, we have far fewer spectra in our sample with a S/N that satisfies the limit of $W_{\text{lim}} = 0.3 \text{ \AA}$. The errors are correspondingly large, and we cannot be sure that the larger $f(\rho)$ values arise merely as a consequence of poor statistics. To emphasise this point, we label in Figure 7 the actual fraction of Mg II detections to the total number sightlines in each bin (as also shown in Fig. 6) for this particular W_{lim} . So for $0 < \rho < 50 \text{ kpc}$, there are only 13 sightlines available, and we detect Mg II in five of them. In the interval $50 < \rho < 100 \text{ kpc}$, we find Mg II in 11 of 33 sightlines. In both cases, the errors are large and compatible with the same values of $f(\rho)$ found for higher W_{lim} .

Searching for Mg II lines near a REW limit of 0.3 \AA introduces potential biases. At high REW limits, the Mg II doublet ratio, $\text{DR} = (W_r \lambda 2796)/(W_r \lambda 2803)$, of detected systems is expected to remain low, close to unity, since both lines are likely to be (close to being) saturated. This means that if a $\lambda 2796$ line is detected at some significance (in our case, at a 2σ level), then the $\lambda 2803$ will often be detected at a similar significance. At a low W_{lim} of 0.3 \AA , however, the Mg II DR is likely to be higher (anywhere between 1.0 and 2.0), and a $\lambda 2796$ line with a strength close to W_{lim} may be detected, but the $\lambda 2803$ line may not be⁶. In our selection process, we required that both members of the doublet be detected at a 2σ significance level, in order to reject lines from other species at different redshifts. This selection process could, in principle, lead us to under-estimate the number of weak systems at low REW limits with $W_r \sim W_{\text{lim}}$. This would then

⁶ Mg II DRs are actually difficult to accurately measure in these SDSS data, since the fractional errors on both of the W_r lines are relatively high, leading to large errors in DR. Although there is a clear trend for systems with $W_r > 0.6 \text{ \AA}$ to have DRs closer to 1.0 , the number of detections for $W_r > 0.3 \text{ \AA}$ is too low to provide a good comparison of DRs between the two samples.

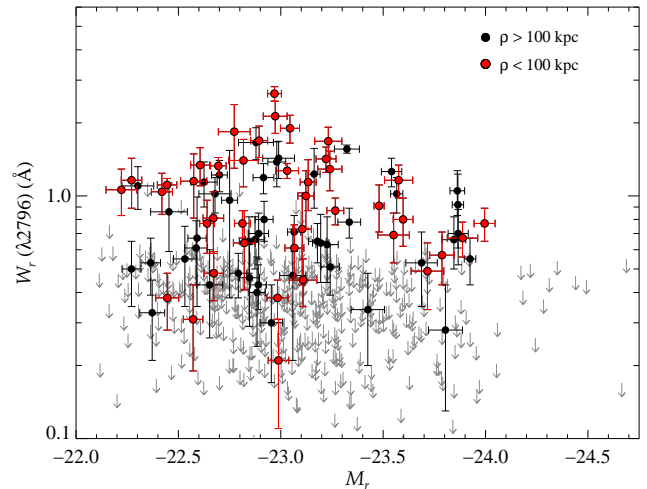


Figure 8. Plot of Mg II $\lambda 2796$ against the absolute magnitude M_r of the galaxies in our sample. Galaxies at impact parameters of $\rho < 100 \text{ kpc}$ are plotted in red, while the remainder are shown in black. K -corrections were calculated for each galaxy using the LRG SED template discussed in §2.3 (assuming no evolution) and z_{CC2} .

increase the difference between $f(\rho)$ for $W_{\text{lim}} = 0.3 \text{ \AA}$ and for higher W_{lim} in Figure 7.

A comparison of $f(\rho)$ for different REW limits with those found by Gauthier et al. (2010) is complicated by the fact that the REW limits may be defined slightly differently for the different analyses; for example, the number of pixels over which a line is measured may be different for each analysis. Although there is a suggestion in our data that $f(\rho)$ changes by a factor of 2 as W_{lim} changes from 0.3 to 0.6 \AA , there is no change in $f(\rho)$ for any increase in W_{lim} when $W_{\text{lim}} > 0.6 \text{ \AA}$. Gauthier et al also see an increase in $f(\rho)$ by a factor of 2, but for different REW limits, 0.5 and 1.0 \AA . It is possible that we are seeing the same change, and that the values of W_{lim} are different simply because of the differences in the way REWs are measured. We find it hard to understand, however, why the differences in W_{lim} should be so large, particular since both analyses use SDSS error arrays and 2σ limits. We also continue to see the sharp decline in $f(\rho)$ beyond 200 kpc , which Gauthier et al do not see for both $W_{\text{lim}} = 0.5$ and 1.0 \AA .

Figure 8 plots the REW of detected Mg II absorption lines, or limits, against the absolute magnitude of the galaxies. In this case, the absolute magnitude is K -corrected to a redshift of zero (as opposed to a rest frame of $z = 0.2$ discussed in §2.3). The figure shows no clear relationship between the luminosity of a galaxy and the REW of Mg II when detected. The figure also shows the Mg II detections segregated by ρ , with galaxies associated with Mg II detections at $\rho < 100 \text{ kpc}$ shown as red circles, and galaxies with associated absorption at $\rho > 100 \text{ kpc}$ shown as black circles. Again, there is no obvious difference between the two groups.

The distribution of the difference between the photometric redshift of the galaxy, z_{CC2} , and the absorption redshift z_{abs} of the Mg II system, $\Delta v = c\Delta z/(1+z_{\text{CC2}})$, is shown in Figure 9. We do not expect this distribution to have a high enough velocity resolution to distinguish between absorption from individual LRG halos, or absorption from lower mass halos that cluster around the larger mass LRG halos (for example). Indeed, although there is some suggestion that the values of Δv

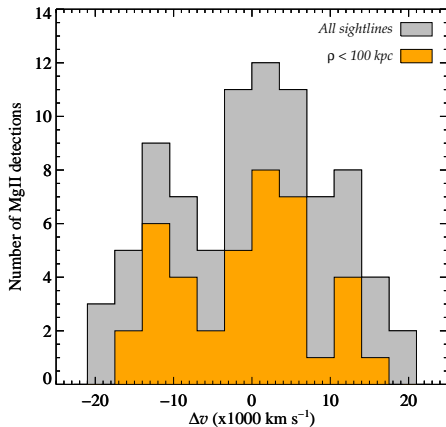


Figure 9. Histogram of the difference between the photometric redshift of the galaxy, z_{CC2} , and the absorption redshift z_{abs} of the Mg II system, when detected. The grey histogram shows the distribution for all sightlines where Mg II is detected, whereas the orange histogram shows the distribution for those pairs with $\rho < 100$ kpc.

tend to cluster around zero km s^{-1} , any peak to the distribution is poorly defined, as we would expect given the photo- z error associated with z_{CC2} . A plot of Δv against ρ (not shown here) also shows no convincing evidence that Δv increases with ρ .

4. DISCUSSION

In this paper, we have constructed a sample of QSO-galaxy pairs from SDSS DR6 based on galaxies having photometric redshifts of between $z = 0.46 - 0.6$, and with small photometric-redshift errors of ~ 0.05 . These photo- z s are taken directly from the SDSS database, and are based on work described by Oyaizu et al. (2008). Due largely to selecting galaxies with small photo- z errors, as well as needing to use galaxies with magnitudes near the detection limit of the SDSS imaging data, we have selected a sample made up primarily of LRG galaxies, as defined by their colors and luminosities. We have searched for Mg II absorption in the SDSS spectra of the background QSOs over a window $\Delta z = \pm 0.1$ of the photo- z of the galaxies. Our most significant result is that the detection of a Mg II system by an LRG is rare, even at small impact parameters of $\rho < 100$ kpc. A simple calculation of the covering fraction as a function of ρ suggest that the probability of detecting strong ($W_r > 0.6 \text{ \AA}$) lines within $\approx 20 - 100 \text{ kpc}^7$ of an LRG is only 10–15%.

4.1. The Role of Unseen Interlopers

Interpreting the covering fraction $f(\rho)$ requires some care. The most obvious question is whether or not the covering fractions shown represent only lower limits to the true values of $f(\rho)$. For a galaxy at any particular ρ , if Mg II is not detected, then the result is clear: the absence of absorption is completely valid for the LRG, even if there exists another galaxy at a similar redshift which lies closer to the QSO sightline. Under the assumption that the photo- z of the galaxy is correct, then the absence of absorption from that galaxy is unambiguous.

⁷ This lower limit of 20 kpc is set by the SDSS’s ability to separate QSOs and galaxies in the imaging data; 20 kpc at $z = 0.5$ correspond to an angular separation of 3.3 arcsec. We implicitly assume that LRGs have not been probed at radii less than 20 kpc in this work.

However, when Mg II is detected, our selection process does not rule out the possibility that another galaxy lies closer to the sightline and is actually responsible for the absorption. Conventionally, surveys to find absorbing galaxies are conducted with the aim of identifying all galaxies in a field, to some stated magnitude limit and impact parameter. In our survey, selecting galaxies based solely on having small errors in their photo- z s does not take into account the possibility that a galaxy exists closer to the sightline, and may be causing the absorption. Late-type sub- L^* galaxies are not easily detected in SDSS imaging data at the redshifts of the LRGs: assuming $M_r^* = -21.2$ (Blanton et al. 2003) a late-type L^* with a flat continuum below a rest-frame wavelength of 4000 \AA (for which a negligible K -corrections would be required) would have an observed magnitude of $r \simeq 21$ at $z = 0.5$, about 1 mag brighter than the detection limit of the SDSS. A visual inspection of the fields around the QSO-LRG pairs in the SDSS data shows that the LRGs are often accompanied by very faint galaxies with intermediate colors, some of which may even lie closer to the QSO than the LRG. Unfortunately, these objects have either no photo- z s, or photo- z s with very large errors, making it difficult to generalize about their association with the identified LRGs. In some fields, the faintest objects are not identified in the SDSS database, and even less-faint galaxies are not detected if they overlap the QSO itself. An example of this can be seen in Figure 2; although the LRG galaxy J112013.16+671116.2 lies only 38 kpc from the QSO J112012.11+671115.9, a galaxy can be seen due south of the sightline which is overlapping the QSO sightline. The galaxy is not cataloged by SDSS, and no photometric information is available. Mg II is detected at the redshift of the LRG galaxy, but whether this, or the interloping galaxy is responsible for the absorption, is not known. The galaxy may be unrelated to the LRG, or could be interacting with it. Without more precise redshift information for all the galaxies in the field, and deeper, higher resolution images, an understanding of this absorption system is far from complete. Finally, we note that the presence of other faint galaxies close to a given QSO-LRG pair is not simply confined to fields where Mg II is detected. Fields where Mg II is not detected are sometimes equally complicated.

If other, gas-rich galaxies closer to the QSO sightlines than the LRGs are indeed responsible for detected Mg II absorption, then our association of absorption systems with the LRG would, obviously, be erroneous, and would provide incorrect information on the absorbing characteristics of LRGs. In Figures 6 and 7, therefore, we would need to remove such sightlines from the appropriate ρ bin. As this would lead to a lower fraction of detected absorption to total sightlines, we would infer that the observed $f(\rho)$ were only upper limits to the true value of $f(\rho)$ for LRGs.

Our inability to identify potential interlopers is the necessary trade-off needed to study large numbers of galaxies using their photometric redshifts instead of completing expensive redshift surveys of many individual fields. Instead of considering which galaxies are nearest to a sightline, an alternative approach to analyzing our data might be to simply estimate the probability of finding Mg II absorption around any LRG, regardless of its environment. The plots of $f(\rho)$ in Figures 6 and 7 effectively measure this probability, if we add back all the LRGs that were excluded because another LRG had been identified closer to the sightline (§3). In fact, leaving in these LRGs makes practically no difference to $f(\rho)$; of the

23 LRGs that have an LRG closer to a line of sight (and for which $W_{\text{lim}} \leq 0.6 \text{ \AA}$) only five show associated Mg II, but their impact parameters are between 90–183 kpc, a range of ρ that is dominated by non-detections of Mg II. This small number of detections adds a negligible amount to $f(\rho)$ over this range.

4.2. Possible Reasons for the Lack of Mg II Absorption

As discussed in §1, LRGs are believed to inhabit some of the highest over-dense regions in the Universe. In Halo Occupation Distribution (HOD) models, they reside in massive halos with DM masses of $10^{13-14} M_{\odot}$, and are usually the central galaxies of rich groups and clusters (Zheng et al. 2009). These high masses have been confirmed through weak lensing measurements by Mandelbaum et al. (2006). Ho et al. (2009) have shown that X-ray luminous clusters with virial masses of $1-5 \times 10^{14} M_{\odot}$ at $z \sim 0.2-0.6$ contain LRGs, and that the brightest LRGs lie at the centers of the clusters. Other LRGs within a cluster, however, need not be found near a cluster’s center.

A simple explanation for the lack of Mg II from galaxies in our sample is that the gas in the halos of LRGs is too hot to sustain clouds cool enough to produce Mg II absorption. High mass halos are traditionally expected to gain gas through “hot mode” accretion, whereby gas from the IGM is accreted into DM halos and is shock heated to its virial temperature, $\sim 10^{7-8} \text{ K}$ for the most massive cluster halos (e.g. Rees & Ostriker 1977; White & Rees 1978; White & Frenk 1991). Additional feedback mechanisms, such as supernovae driven winds, or AGN accretion, can help maintain high gas temperatures around galaxies in massive halos (see, e.g. the review by Baugh 2006). For gas that is collisionally ionized and in thermal equilibrium, most magnesium is in the form of Mg III at 10^5 K (Sutherland & Dopita 1993). Lower mass halos hosting $\sim L^*$ galaxies also have virial temperatures that are too high for Mg II to dominate the ion fraction (Fukugita & Peebles 2006), but models in which cool photoionized gas can survive in the hot halo are able to reproduce many of the characteristics of Mg II (and other ion) systems (e.g. Mo & Miralda-Escude 1996). Semi-analytical models and numerical simulations of gas hydrodynamics in CDM constructs also find that cool gas can exist in galaxy halos through “cold mode” accretion, which occurs when gas [with, e.g., $T < 2.5 \times 10^5 \text{ K}$ in Kereš et al. (2009)] is funnelled from the IGM down filaments into the halos. This process is expected to dominate in low mass ($< 10^{11-12} M_{\odot}$) halos (Birnboim & Dekel 2003; Katz et al. 2003; Kereš et al. 2005; Birnboim et al. 2007; Kereš et al. 2009).

Several investigators have considered whether the masses of Mg II absorbing halos are consistent with those expected for the existence of Mg II absorbing clouds. Bouché et al. (2006) cross-correlated Mg II absorption systems detected in SDSS spectra with a catalog of LRGs (with photo- z s), from which they were able to measure a mean halo mass 20–40 times smaller than LRG halos. They found that the halo mass was *anti-correlated* with Mg II equivalent width, and hence that the absorbing clouds were not virialized in the halo. This result was unexpected, since more massive virialized halos, with brighter galaxies, should have absorbing gas clouds with larger velocity dispersions. Since the equivalent width of a Mg II line is, to first order, proportional to the number of narrow components comprising the line (at least for strong lines), then (assuming that Mg II absorption is directly related to clouds within a galactic halo), W_r should be proportional

to the virial velocity of gas in the halo, and hence to halo mass. Bouché et al. estimated the mass of halos in which strong ($W_r > 1 \text{ \AA}$) Mg II was found to be $\approx 10^{12} M_{\odot}$, and determined that an anti-correlation existed between halo mass M_h and W_r . Lundgren et al. (2009) refined these values with additional SDSS data releases, and determined that Mg II absorbers with $W_r \geq 1.4 \text{ \AA}$ arose in halo masses of $10^{11.3} M_{\odot}$, while absorbers with $0.8 \leq W_r \leq 1.4 \text{ \AA}$ arose in halos with $M_h \sim 10^{12.7} M_{\odot}$.

Our results are in broad agreement with this anti-correlation of W_r and M_h , in the sense that we find few Mg II systems in the high mass halos of LRGs. Bouché et al. did not predict a covering factor for a given halo mass, making it difficult for us to compare in detail our results with their models. In interpreting their results, Bouché et al. favored the explanation that galactic outflows within the halos caused the majority of Mg II systems, and not infalling IGM gas. In keeping with this hypothesis, we would say that we see little Mg II absorption because few star-forming galaxies exist in high mass groups and clusters. The LRGs in our sample are likely to be cluster ellipticals, with little significant star formation or outflowing cool gas. We return to this point below.

Tinker & Chen (2008) and Chen & Tinker (2008) modelled Mg II absorbing halos in terms of the HOD formalism, and found that in order to reproduce the anti-correlation of W_r and M_h seen by Bouché et al., their models needed to incorporate a transitional halo mass at which shock heated gas becomes more dominant in higher mass halos, leading to less Mg II absorption. In these models, the halos of Mg II absorbing galaxies have masses of $\sim 10^{11-13} M_{\odot}$, with a transitional mass of $10^{11.6} M_{\odot}$, a result consistent with the simulations of cold-mode accretion of gas into galaxy centers. Again, in the context of our survey, the absence of Mg II near LRGs is because they reside in halos that are too massive to support cool Mg II clouds.

In detail, it is less clear whether our results are compatible with Tinker & Chen’s models, which were calculated for halo masses as high as $10^{14} M_{\odot}$. They found that “a significant fraction of cluster-sized halos contain some cold gas with a high covering factor”, although they noted that the constraints on their models were poor for halo masses $> 10^{13} M_{\odot}$. If we take all the LRGs in our sample to represent cluster-sized halos, our results would tend to argue against these findings. We would say that our sample shows that a significant fraction of cluster-size halos contain cold gas with a low covering factor, or, alternatively, only a few cluster-size halos contain cold gas with a high covering factor.

4.3. Possible Origins for Observed Mg II Absorption

Despite the fact that most LRGs do not cause Mg II absorption, we have shown that even after removing a contribution to the number of detections that arise from chance along any sightline, there are still a small number of Mg II systems associated with the identified galaxies. In this section we discuss possible origins for these systems.

Could the few Mg II systems we see around LRGs arise from the small amounts of cool gas that remain in galactic halos? Cold-mode accretion is expected to be a dominate channel for galaxies at high redshifts, or low-mass galaxies at lower redshifts. As indicated above, the halo masses of LRGs are likely to be several dex above the transition mass between the hot and cold mode regimes ($10^{11-12} M_{\odot}$), so cold accretion is unlikely to be significant. At $z=0$, numerical sim-

ulations suggest that the fraction of gas in halos with masses of $10^{13}M_{\odot}$ and temperatures $< 2.5 \times 10^5$ K is only a few percent, although whether cold filamentary streams reaching into the halo cores at $z \sim 0.5$ are able to survive is unclear (Kereš et al. 2009). The problem with this speculation is that we do not actually know the mass distribution of the LRGs we have sampled. Without a better measurement of the LRGs masses and environments, it is difficult to compare our results with simulations and determine whether even small amounts of cold gas might be associated with the LRGs we have studied.

A different explanation is that Mg II absorption might arise in the disks of interloping late-type galaxies which inhabit the outer regions of the LRG groups and clusters (e.g. Hansen et al. 2009, and refs. therein). Any difference in the redshifts between an LRG and another cluster or group member will be much smaller than the error in the photometric redshift of the LRG, and will not be detectable in Figure 9. The morphologies of galaxies are known to change from late to early type as the distance to the center of a cluster decreases, and late-types may only need to present a small cross-section to account for the low covering factor seen in Figure 6. Moreover, the transformations that take place in late-type galaxies in the environment of rich groups and clusters offer plausible mechanisms for increasing their Mg II cross-section; tidal interactions with other cluster galaxies, or stripping of galactic ISMs by the intracluster medium, can re-distribute cool gas over larger areas than those covered by single galaxy disks. The problem with this scenario, however, is that we would expect the surface density of late-type galaxies (as a function of the projected distance from the center of a cluster) to be relatively constant over Mpc scales⁸; there is no obvious reason why the number of spiral galaxies would decline to zero at impact parameters of 200 kpc from an LRG. Put another way, if late-type galaxies at the outer regions of galaxies clusters were responsible for detected Mg II systems, we would expect the number of systems “accidentally” intercepted by QSO sightlines through a cluster to be largely constant between 20 and 200 kpc of an LRG, possibly at a level slightly higher than the background Mg II systems discussed in §3. Since this is not what we observe, we consider this scenario an unlikely explanation for the few Mg II systems we do detect.

A more likely explanation is that the Mg II systems arise as a consequence of wet mergers between LRGs and gas-rich satellites, with the latter providing fuel for star formation in the former. If hierarchical merger models are correct, LRGs should certainly have the most vigorous merger histories of galaxies in the Universe. Again, galaxy-galaxy interactions, or galaxy cannibalism, is a good way to distribute tidal debris over areas of the sky larger than those of individual galactic disks. Absorption from tidally disrupted gas would also explain the large Mg II equivalent widths, since the kinematics of the interacting galaxies could spread Mg II components over large velocity intervals (e.g. Bowen et al. 1994). More importantly, however, if Mg II systems are more closely associated with star forming galaxies, as discussed in §1, where galactic outflows push cool gas out of galactic disks, then perhaps LRGs that have undergone recent bursts of star formation may be responsible for strong Mg II absorption lines. Again, outflows from star-forming galaxy disks would explain the strong Mg II equivalent widths (e.g. Chelouche & Bowen

2010, and refs. therein).

The star formation history of LRGs has been studied by several authors. Eisenstein et al. (2003) found that 10% of the SDSS LRG population have significant [O II] emission, while Roseboom et al. (2006) found that 12.5% of $L > 3L^*$ LRGs have spectra with some combination of [O II] emission lines and strong H δ absorption lines, indicative of on-going, or recent, star formation. The similarity between this fraction of LRGs, and the fraction we find associated with Mg II absorption, is striking. Excluding their [O II] emission-only subset of galaxies, $\simeq 4\%$ of Roseboom et al.’s LRGs show good evidence for star formation; as noted by both Eisenstein et al. and Roseboom et al., the detection of emission lines alone without corroborating absorption features is ambiguous, since [O II] can arise from galaxies with AGN activity (such as LINERS), rather than from star formation. The Mg II absorption cross-section of AGN has not been studied in detail, although QSOs at similar redshifts to the LRGs in our sample are known to show high Mg II covering factors ($\sim 90\%$) out to ~ 100 kpc for lines with $W_r > 0.5 \text{ \AA}$ (Bowen et al. 2006, 2011). Of course, QSO and AGN activity may itself be triggered by galaxy mergers (see, e.g. Hopkins et al. 2008, and refs therein), a process which distributes gas over a wide cross-section, triggers high star formation (Mihos & Hernquist 1996), and causes gas to be expelled from the galaxy through supernovae driven winds (Springel et al. 2005). Hence we may be seeing Mg II from the same combination of star-forming and (perhaps) AGN LRGs as those selected by Roseboom et al. and Eisenstein et al., leading to the same fraction of Mg II absorbers. Roseboom et al. were unable to settle on the physical mechanisms which might produce star-forming/AGN LRG galaxies, but noted that their existence was consistent with Λ CDM cosmologies that included mergers of gas-rich galaxies, and cooling at the centers of clusters, much as already discussed above. Obviously, whether the LRG galaxies in our sample show any signs of the same star formation or AGN activity seen by Eisenstein et al. and Roseboom et al. can be tested by simply recording the spectra of the LRGs. Gauthier et al. (2010) have begun a spectroscopic follow-up of their LRGs, but so far, only one galaxy associated with Mg II absorption and at an impact parameter < 100 kpc has been observed. Its SED shows no obvious signs of star-formation or AGN activity.

Whether Mg II absorption originates in tidal debris from merging galaxies, or whether it arises in outflows from star formation *instigated* by merging galaxies, in both cases the processes involve the interaction of galaxies. Unfortunately, at redshifts of ~ 0.5 , measuring the rate of even *major* LRG mergers, where both interactors might be bright enough to be visible in large-area sky surveys, has proved difficult; the rate though, does appear to be low (Masjedi et al. 2008; Bundy et al. 2009; De Propris et al. 2010, and refs therein). The comoving volume density of the most massive ($M > \sim 10^{11}M_{\odot}$) galaxies changes little at $z \sim 0.2 - 1$. The numbers are not increasing [at least to within factors of 2–3 — see, e.g. Conselice et al. (2007)], even though more would be expected to arise at lower- z if they continued to accrete galaxies through mergers.

At much lower redshifts, $z \simeq 0.02 - 0.14$, where galaxy environment is easier to map in shallow galaxy surveys, Huang & Gu (2009) found that 5% of bright (between M_r of -20 and -24 , so similar to the LRGs) E and S0 galaxies showed signs of on-going or recent star formation, and an additional

⁸ For example, the mean radius at which the galaxy density is defined to be 200 times the field density (R_{200}) is usually given to be $\simeq 1$ Mpc.

10–13% showed LINER or Seyfert activity. These numbers are similar to those measured specifically for the LRGs by Roseboom et al. Unfortunately, Huang & Gu excluded galaxies with disturbed morphologies, making it hard to know how much star formation in early-type galaxies might be associated with merging systems. Interestingly, the environments of their star-forming ellipticals appear to be quite mixed. Although 5 galaxies seem to be relatively isolated, 8 of the 13 listed by Huang & Gu have one or more neighbors with similar redshifts within 300 kpc and/or have been associated with galaxy groups or clusters by other authors. Hence at low- z it seems plausible that a small number of bright, star-forming ellipticals can be found in similar dense environments to those of LRGs at higher- z .

Can we measure any difference in the environment of those LRGs that we associate absorption with and those that show no absorption? To investigate this question, we collated all galaxies within 5 arcmin of every QSO sightline in our survey from the SDSS DR7 GALAXY database. At $z = 0.6$, 5 arcmins corresponds to a proper length of 2 Mpc, which approximates cluster-like scales. We calculated the number of galaxies per shell along each sightline, $n(r)$, where we counted galaxies in shells of width 50 arcsec, and then compared both the average and median of $n(r)$ for all sightlines with and without Mg II detections. We took the error in these values to be the measured standard deviation in $n(r)$. In one case we counted all galaxies, regardless of their redshifts; in a second case, we used only red galaxies that satisfied the color selection of Cannon et al. (2006) discussed in §2.3 and shown in Figure 3. In the latter case, these red galaxies are more likely to be at the redshifts of the previously selected LRGs.

For both galaxy samples, unfortunately, we could not differentiate between the average or median of $n(r)$ for sightlines with and without Mg II absorption. We found that the variance in the number of galaxies per field dominates the distribution of $n(r)$ for both absorbers and non-absorbers. In particular, having only 85 unique QSO sightlines showing Mg II detection provides too small a sample to show any difference with the distribution of galaxies in the 482 QSO fields that show no Mg II. A larger study which matches all LRG environments around all QSO sightlines, and not just QSOs with LRGs within 30 arcsec of a sightline (as used in this study), may be more fruitful, but is beyond the scope of this paper.

Our search for Mg II absorption lines from LRGs can only be used so far in interpreting the origin of QSO absorption line systems. The lack of Mg II from this population of galaxies suggests that the majority of Mg II systems have little to do with massive red galaxies, nor probably, massive hot halos. The implication is that if Mg II systems are indeed associated with galaxies (and are not simply metal-enriched intergalactic clouds) then other types of galaxies and environments are primarily responsible for Mg II absorption. This is hardly a surprising conclusion, given the identification of the strong links between Mg II systems and late-type, star-forming galaxies discussed in the Introduction of this paper. Indeed, as our understanding of galaxy properties and galaxy number counts has become more refined, and with a more precise counting of Mg II systems at the lowest redshifts, it has become easier to account for the origin of *all* Mg II systems by star forming disk galaxies (e.g. Chelouche & Bowen 2010, and refs therein). Whether the small percentage of Mg II absorbers found herein to be associated with LRGs provides any deeper insights into the origin of Mg II systems, is not clear.

D.V.B is funded through LTSA NASA grant NNG05GE26G. D.C acknowledges support from a Marie Curie grant PIRG06-GA-2009-256434. We thank FG and Chuli for their continuing support. This paper is dedicated to the memory of FG. Funding for the SDSS and SDSS-II has been provided by the Alfred P. Sloan Foundation, the Participating Institutions, the National Science Foundation, the U.S. Department of Energy, the National Aeronautics and Space Administration, the Japanese Monbukagakusho, the Max Planck Society, and the Higher Education Funding Council for England. The SDSS Web Site is <http://www.sdss.org/>.

The SDSS is managed by the Astrophysical Research Consortium for the Participating Institutions. The Participating Institutions are the American Museum of Natural History, Astrophysical Institute Potsdam, University of Basel, University of Cambridge, Case Western Reserve University, University of Chicago, Drexel University, Fermilab, the Institute for Advanced Study, the Japan Participation Group, Johns Hopkins University, the Joint Institute for Nuclear Astrophysics, the Kavli Institute for Particle Astrophysics and Cosmology, the Korean Scientist Group, the Chinese Academy of Sciences (LAMOST), Los Alamos National Laboratory, the Max-Planck-Institute for Astronomy (MPIA), the Max-Planck-Institute for Astrophysics (MPA), New Mexico State University, Ohio State University, University of Pittsburgh, University of Portsmouth, Princeton University, the United States Naval Observatory, and the University of Washington.

REFERENCES

- Bahcall, J. N., Jannuzi, B. T., Schneider, D. P., Hartig, G. F., & Jenkins, E. B. 1992, *ApJ*, 398, 495
- Banerji, M., Ferreras, I., Abdalla, F. B., Hewett, P., & Lahav, O. 2010, *MNRAS*, 24
- Barton, E. J. & Cooke, J. 2009, *AJ*, 138, 1817
- Baugh, C. M. 2006, *Reports on Progress in Physics*, 69, 3101
- Bechtold, J. & Ellingson, E. 1992, *ApJ*, 396, 20
- Bergeron, J. 1986, *A&A*, 155, L8
- Bergeron, J. & Boisse, P. 1991, *A&A*, 243, 344
- Bergeron, J., Kunth, D., & D’Odorico, S. 1987, *A&A*, 180, 1
- Birnboim, Y. & Dekel, A. 2003, *MNRAS*, 345, 349
- Birnboim, Y., Dekel, A., & Neistein, E. 2007, *MNRAS*, 380, 339
- Blades, J. C., Hunstead, R. W., & Murdoch, H. S. 1981, *MNRAS*, 194, 669
- Blanton, M. R., et al, 2003, *ApJ*, 592, 819
- Blanton, M. R. & Roweis, S. 2007, *AJ*, 133, 734
- Boksenberg, A., Danziger, I. J., Fosbury, R. A. E., & Goss, W. M. 1980, *ApJ*, 242, L145
- Boksenberg, A. & Sargent, W. L. W. 1978, *ApJ*, 220, 42
- Borthakur, S., Tripp, T. M., Yun, S. Y., Momjian, E., Meiring, J. D., Bowen, D. V., & York, D. G. 2010, *ApJ*, in prep
- Bouché, N., Murphy, M. T., Péroux, C., Csabai, I., & Wild, V. 2006, *MNRAS*, 371, 495
- Bouché, N., Murphy, M. T., Péroux, C., Davies, R., Eisenhauer, F., Förster Schreiber, N. M., & Tacconi, L. 2007, *ApJ*, 669, L5
- Bowen, D. V., Blades, J. C., & Pettini, M. 1995, *ApJ*, 448, 634
- . 1996, *ApJ*, 472, L77
- Bowen, D. V., Chelouche, D., Ménard, B., York, D. G., Inada, N., Oguri, M., Strauss, M. A., & Brandt, W. N. 2011, *ApJ*, in prep
- Bowen, D. V., Hennawi, J. F., Ménard, B., Chelouche, D., Inada, N., Oguri, M., Richards, G. T., Strauss, M. A., Vanden Berk, D. E., & York, D. G. 2006, *ApJ*, 645, L105
- Bowen, D. V., Pettini, M., Penston, M. V., & Blades, C. 1991, *MNRAS*, 249, 145
- Bowen, D. V., Roth, K. C., Blades, J. C., & Meyer, D. M. 1994, *ApJ*, 420, L71
- Brooks, A. M., Governato, F., Quinn, T., Brook, C. B., & Wadsley, J. 2009, *ApJ*, 694, 396
- Brown, M. J. I., Dey, A., Jannuzi, B. T., Brand, K., Benson, A. J., Brodwin, M., Croton, D. J., & Eisenhardt, P. R. 2007, *ApJ*, 654, 858
- Bundy, K., Fukugita, M., Ellis, R. S., Targett, T. A., Belli, S., & Kodama, T. 2009, *ApJ*, 697, 1369

- Cannon, R., et al, 2006, MNRAS, 372, 425
 Charlton, J. C. & Churchill, C. W. 1996, ApJ, 465, 631
 Chelouche, D. & Bowen, D. V. 2010, ApJ, 722, 1821
 Chen, H., Helsby, J. E., Gauthier, J., Shectman, S. A., Thompson, I. B., & Tinker, J. L. 2010, ApJ, 714, 1521
 Chen, H.-W. & Tinker, J. L. 2008, ApJ, 687, 745
 Coleman, G. D., Wu, C., & Weedman, D. W. 1980, ApJS, 43, 393
 Conselice, C. J., et al, 2007, MNRAS, 381, 962
 Cool, R. J., Eisenstein, D. J., Fan, X., Fukugita, M., Jiang, L., Maraston, C., Meiksin, A., Schneider, D. P., & Wake, D. A. 2008, ApJ, 682, 919
 Cristiani, S. 1987, A&A, 175, L1
 De Propriis, R., Driver, S. P., Colless, M., Drinkwater, M. J., Loveday, J., Ross, N. P., Bland-Hawthorn, J., York, D. G., & Pimblett, K. 2010, AJ, 139, 794
 Eisenstein, et al, 2001, AJ, 122, 2267
 Eisenstein, D. J., et al, 2003, ApJ, 585, 694
 Ferreras, I., Lisker, T., Pasquali, A., Khochfar, S., & Kaviraj, S. 2009, MNRAS, 396, 1573
 Fukugita, M. & Peebles, P. J. E. 2006, ApJ, 639, 590
 Gauthier, J., Chen, H., & Tinker, J. L. 2009, ApJ, 702, 50
 —. 2010, ApJ, 716, 1263
 Hansen, S. M., Sheldon, E. S., Wechsler, R. H., & Koester, B. P. 2009, ApJ, 699, 1333
 Ho, S., Lin, Y., Spergel, D., & Hirata, C. M. 2009, ApJ, 697, 1358
 Hogg, D. W., et al, 2002, AJ, 124, 646
 Hopkins, P. F., Hernquist, L., Cox, T. J., & Kereš, D. 2008, ApJS, 175, 356
 Huang, S. & Gu, Q. 2009, MNRAS, 398, 1651
 Katz, N., Keres, D., Dave, R., & Weinberg, D. H. 2003, in *Astrophysics and Space Science Library*, Vol. 281, *The IGM/Galaxy Connection. The Distribution of Baryons at $z = 0$* , ed. J. L. R. . M. E. Putman, 185
 Kaufmann, T., Bullock, J. S., Maller, A. H., Fang, T., & Wadsley, J. 2009, MNRAS, 396, 191
 Kereš, D., Katz, N., Fardal, M., Davé, R., & Weinberg, D. H. 2009, MNRAS, 395, 160
 Kereš, D., Katz, N., Weinberg, D. H., & Davé, R. 2005, MNRAS, 363, 2
 Le Brun, V., Bergeron, J., Boisse, P., & Christian, C. 1993, A&A, 279, 33
 Lundgren, B. F., et al, 2009, ApJ, 698, 819
 Lupton, R., Blanton, M. R., Fekete, G., Hogg, D. W., O'Mullane, W., Szalay, A., & Wherry, N. 2004, PASP, 116, 133
 Mandelbaum, R., Seljak, U., Cool, R. J., Blanton, M., Hirata, C. M., & Brinkmann, J. 2006, MNRAS, 372, 758
 Martin, C. L. 1999, ApJ, 513, 156
 —. 2005, ApJ, 621, 227
 Masjedi, M., Hogg, D. W., & Blanton, M. R. 2008, ApJ, 679, 260
 Ménard, B., Wild, V., Nestor, D., Quider, A., & Zibetti, S. 2010, arXiv:0912.3263
 Mihos, J. C. & Hernquist, L. 1996, ApJ, 464, 641
 Mo, H. J. & Miralda-Escude, J. 1996, ApJ, 469, 589
 Nestor, D. B., Turnshek, D. A., & Rao, S. M. 2005, ApJ, 628, 637
 Norman, C. A., Bowen, D. V., Heckman, T., Blades, C., & Danly, L. 1996, ApJ, 472, 73
 Noterdaeme, P., Srianand, R., & Mohan, V. 2010, MNRAS, 108
 Oyaizu, H., Lima, M., Cunha, C. E., Lin, H., Frieman, J., & Sheldon, E. S. 2008, ApJ, 674, 768
 Rees, M. J. & Ostriker, J. P. 1977, MNRAS, 179, 541
 Roseboom, I. G., et al, 2006, MNRAS, 373, 349
 Rupke, D. S. & Veilleux, S. 2005, ApJ, 631, L37
 Schwartz, C. M. & Martin, C. L. 2004, ApJ, 610, 201
 Sembach, K. R. & Savage, B. D. 1992, ApJS, 83, 147
 Springel, V., Di Matteo, T., & Hernquist, L. 2005, MNRAS, 361, 776
 Steidel, C. C. 1993, in *ASSL Vol. 188: The Environment and Evolution of Galaxies*, 263
 Steidel, C. C. 1995, in *QSO Absorption Lines, Proceedings of the ESO Workshop Held at Garching, Germany, 21 - 24 November 1994*, ed. G. Meylan. Springer-Verlag Berlin Heidelberg, New York, 139
 Steidel, C. C., Dickinson, M., & Persson, S. E. 1994, ApJ, 437, L75
 Steidel, C. C., Kollmeier, J. A., Shapley, A. E., Churchill, C. W., Dickinson, M., & Pettini, M. 2002, ApJ, 570, 526
 Strickland, D. K., Heckman, T. M., Colbert, E. J. M., Hoopes, C. G., & Weaver, K. A. 2004a, ApJS, 151, 193
 —. 2004b, ApJ, 606, 829
 Sutherland, R. S. & Dopita, M. A. 1993, ApJS, 88, 253
 Tinker, J. L. & Chen, H. 2008, ApJ, 679, 1218
 Tremonti, C. A., Moustakas, J., & Diamond-Stanic, A. M. 2007, ApJ, 663, L77
 Tripp, T. M. & Bowen, D. V. 2005, in *IAU Colloq. 199: Probing Galaxies through Quasar Absorption Lines*, 5–23
 Wagoner, R. V. 1967, ApJ, 149, 465
 Wake, D. A., et al, 2006, MNRAS, 372, 537
 Weiner, B. J., et al, 2009, ApJ, 692, 187
 White, S. D. M. & Frenk, C. S. 1991, ApJ, 379, 52
 White, S. D. M. & Rees, M. J. 1978, MNRAS, 183, 341
 Wild, V., Hewett, P. C., & Pettini, M. 2007, MNRAS, 374, 292
 Womble, D. S., Junkkarinen, V. T., Cohen, R. D., & Burbidge, E. M. 1990, AJ, 100, 1785
 Yanny, B., York, D. G., Hamilton, D., Schommer, R. A., & Williams, T. V. 1987, ApJ, 323, L19
 York, e. a. 2000, AJ, 120, 1579
 Zheng, Z., Zehavi, I., Eisenstein, D. J., Weinberg, D. H., & Jing, Y. P. 2009, ApJ, 707, 554
 Zibetti, S., Ménard, B., Nestor, D. B., Quider, A. M., Rao, S. M., & Turnshek, D. A. 2007, ApJ, 658, 161

Table 1
Mg II Absorption in QSO-galaxy pairs

QSO (1)	Plate-MJD-fibre (2)	z _{QSO} (3)	Galaxy (4)	z _{CG2} (5)	<i>r</i> (6)	<i>M_r</i> (7)	θ ($''$) (8)	ρ (kpc) (9)	<i>z</i> _{abs} (10)	Δz (km s ⁻¹) (11)	<i>W_r</i> (Mg II)	
											$\lambda 2796$ (Å) (12)	$\lambda 2803$ (Å) (13)
J010601.41-083556.8	0659-52199-361	1.384	J010601.17-083557.0	0.476 ± 0.028	19.7	-23.1	3.4	20.0	< 0.57	< 0.57
J123744.56+110658.2	1233-52734-443	0.946	J123744.60+110654.3	0.469 ± 0.046	20.7	-22.0	3.9	23.0	< 0.30	< 0.30
J122922.94+495650.5	0971-52644-156	1.600	J122922.71+495653.5	0.508 ± 0.035	20.5	-22.6	3.8	23.3	< 0.73	< 0.74
J115312.76+463553.5	1446-53080-202	1.123	J115312.88+463549.7	0.495 ± 0.039	20.6	-22.4	4.0	24.4	0.4417	0.0532	0.47 ± 0.13	0.14 ± 0.14
J083426.64+291311.1	1268-52933-493	1.558	J083426.37+291313.4	0.562 ± 0.035	20.4	-23.2	4.1	26.8	< 0.48	< 0.49
J160624.23+434336.7	1170-52756-399	1.489	J160624.39+434340.8	0.517 ± 0.023	19.5	-23.7	4.4	27.6	< 0.42	< 0.40
J125929.93+560525.9	1318-52781-203	1.674	J125929.40+560525.2	0.515 ± 0.025	20.1	-23.1	4.5	27.7	< 0.64	< 0.62
J082840.61+364819.0	0827-52312-143	1.376	J082840.92+364815.8	0.462 ± 0.042	20.1	-22.6	5.0	29.2	< 0.23	< 0.24
J102054.61+501007.3	1008-52707-251	1.438	J102054.55+501012.2	0.488 ± 0.038	20.1	-22.8	4.9	29.6	0.4350	0.0531	1.91 ± 0.25	1.25 ± 0.26
J162921.31+160356.8	2207-53558-288	1.010	J162921.50+160352.6	0.479 ± 0.035	19.8	-23.3	5.0	30.0	< 0.63	< 0.63
J143248.46+613817.4	0607-52368-520	2.017	J143248.01+613820.9	0.554 ± 0.029	20.2	-23.3	4.8	31.1	0.6155	-0.0618	0.69 ± 0.28	0.81 ± 0.28
J145307.68+354200.1	1384-53121-354	1.752	J145307.96+354156.4	0.534 ± 0.037	20.8	-22.4	5.0	31.8	< 0.65	< 0.63
J142329.45+020443.0	0534-51997-514	0.961	J142329.36+020437.9	0.491 ± 0.042	20.5	-22.6	5.3	31.8	< 0.40	< 0.41
J140513.91+135219.2	1704-53178-472	1.085	J140513.66+135215.0	0.487 ± 0.036	20.3	-22.6	5.6	33.8	< 0.74	< 0.71
...	J140515.71+135221.4	0.473 ± 0.039	20.7	-22.1	26.4	156.4	< 0.75	< 0.78
...	J140515.43+135235.5	0.491 ± 0.024	19.7	-23.2	27.4	165.9	< 0.67	< 0.72
...	J140514.23+135150.6	0.570 ± 0.026	20.0	-23.7	29.0	189.2	< 0.53	< 0.53
J130351.25+141650.4	1771-53498-064	1.185	J130351.54+141646.8	0.497 ± 0.043	20.3	-22.7	5.6	34.0	< 0.60	< 0.59
...	J130351.41+141718.1	0.464 ± 0.040	20.4	-22.3	27.8	162.9	< 0.79	< 0.81
J091040.04+535427.9	0553-51999-509	1.096	J091040.59+535430.5	0.511 ± 0.031	20.5	-22.6	5.5	34.1	< 0.62	< 0.61
J122522.20+325630.8	2015-53819-247	1.119	J122521.79+325632.9	0.530 ± 0.035	20.3	-23.0	5.5	34.9	0.5246	0.0053	0.72 ± 0.18	1.06 ± 0.17
J132332.32+560339.7	1320-52759-180	1.037	J132333.06+560340.2	0.472 ± 0.025	19.7	-23.0	6.2	36.7	< 0.71	< 0.75

The complete version of this table can be found at <http://www.astro.princeton.edu/~dvb/STHtable.pdf>.

Entries are listed in order of increasing QSO-galaxy impact parameter (col. 9). In some cases, multiple galaxies satisfying our selection criteria were found around a single sightline. These are also listed, but are kept together with a single QSO entry, even though they may have much larger impact parameters. The columns list the following parameters: Col. (1): Background QSO designation. For brevity, the "SDSS" prefix has been dropped from this list, and the list in col. (4); col. (2): spectroscopic fiber identification from DR6; col. (3): emission redshift of QSO; col. (4): galaxy designation; col. (5): galaxy photometric redshift and error; col. (6): galaxy *r*-band model magnitude, de-reddened for Milky Way dust absorption; col. (7): galaxy absolute magnitude, based on z_{CG2}, after applying a *K*-correction to measure the *r*-band luminosity at a redshift *z* = 0; col. (8): angular separation between QSO sightline and galaxy; col. (9): impact parameter between QSO sightline and galaxy; col. (10): Mg II absorption redshift, if doublet detected within ±0.1 of z_{CG2}; col. (11): difference in redshift between z_{abs} and z_{CG2}; cols. (12,13): rest equivalent widths and errors of Mg II lines, when detected, or 2σ upper limit, if absorption lines not detected.